VSP

*Journal of Adhesion Science and Technology 22 (2008) 545–567*

Journal of ADHESION SCIENCE and TECHNOLOGY
www.brill.nl/jast

# Adhesion and Surface Issues in Cellulose and Nanocellulose

**Douglas J. Gardner** [a,*], **Gloria S. Oporto** [a], **Ryan Mills** [a] **and My Ahmed Said Azizi Samir** [b]

[a] University of Maine, Forest Bioproducts Research Initiative and Advanced Engineered Wood Composite (AEWC) Center, University of Maine, Orono, ME 04469, USA

[b] Nanocomposites and Bioconcepts SARL, N170 Tanalt Alhouda, Agadir — Morocco

**Abstract**

This paper provides a review of the scientific literature concerned with adhesion and surface properties of cellulose and nanocellulose. Cellulose is the most abundant chemical compound on earth and its natural affinity for self-adhesion has long been recognized. The ease of adhesion that occurs in cellulose has contributed to its use in paper and other fiber-based composite materials. Cellulose adhesion, which has received considerable attention over the past half century, occurs over a practical length scale ranging from the nanoscale to millimeters. Adhesion theories that have been examined in the bonding of cellulose fibers include: mechanical interlocking, adsorption or wetting theory, diffusion theory, and the theory of weak boundary layers. Cellulose fibers on the nanoscale are prepared in four different ways: (1) bacterial cellulose nanofibers, (2) cellulose nanofibers by electrospinning, (3) microfibrillated cellulose plant cell fibers and (4) nanorods or cellulose whiskers. Structure and properties of nanocellulose that are important include: morphology, crystalline structure, surface properties, chemical and physical properties, and properties in liquid suspension. Cellulosic nanofibers present a very high surface area which makes the adhesion properties the most important parameter to control for nanocomposite applications. In this paper, we will focus on discussion of the adhesion and surface characteristics of cellulose nanofibers that impact its properties and application in nanomaterials.



**Keywords**

Nanotechnology, cellulose, nanocellulose, whiskers, adhesion, bacterial cellulose

## 1. Introduction

Nanotechnology is the understanding and control of matter at dimensions of roughly 1–100 nm, where unique phenomena enable novel applications. Encompassing nanoscale science, engineering and technology, nanotechnology involves imaging, measuring, modeling, and manipulating matter at this length scale. Nanotechnology research and development (R&D) in the US has been high priority

* To whom correspondence should be addressed. Tel.: (1-207) 581-2846. Fax: (1-207) 581-2074; e-mail: douglas.gardner@umit.maine.edu

 DOI:10.1163/156856108X295509

research across all segments of science and engineering since the enactment of the National Nanotechnology Initiative (NNI) in 2001. Nanomaterials derived from renewable biomaterials, especially cellulose and lignocellulose, will undoubtedly play a large role in the nanotechnology research effort. To exploit their potential, R&D investments must be made in the science and engineering that will fully determine the properties and characteristics of cellulose and lignocellulose at the nanoscale, develop the technologies to manipulate self-assembly and multifunctionallity, and develop these new technologies to the point where industry can produce advanced and cost-competitive cellulose and lignocellulose-based products [1].

The behavior of cellulose surfaces in different media as well as their interaction with different chemicals is of great importance in their current and future applications (papermaking, composites and nanocomposites). The mechanical performance of composites, for instance, is dependent on the degree of dispersion of the fibers in the matrix polymer and the nature and intensity of fiber–polymer adhesion interactions. To explain cellulose adhesion phenomena, it is important to review the mechanisms of adhesion. Several theories have been proposed to provide an explanation for adhesion phenomena; however, there is no single theory that explains adhesion in a general, comprehensive way. The bonding phenomenon is the sum of a number of mechanical, physical and chemical forces that overlap and influence each other. Based on this, it is not possible to separate these forces, and adhesion has been characterized as related to mechanical interlocking caused by the mechanical anchoring of the adhesive in the pores and the uneven parts of the surface; electrostatic forces, as they relate to the difference in electonegativities of adhering materials; diffusion which is related to the interpenetration of molecular chains at the interface where the adhesive and surface being bonded interact; weak boundary layers referring to the accumulation of air bubbles or low-molecular-weight compounds from the adhesive, the adherends or the surroundings at the interface; and adsorption and wetting which are related to highly localized intermolecular forces. Wetting may be attributed to acid–base interactions, weak hydrogen bonding or van der Waals forces (dipole–dipole and dispersion forces). The extent of wetting depends on the differences in surface free energies of the solid, liquid and subsequent interface.

## 2. Cellulose Structure and Properties

Cellulose is a homopolymer composed of $\beta$-D-glucopyranose units which are linked together by $(1 \rightarrow 4)$-glycosidic bonds [2]. The length of a native cellulose molecule is at least 5000 nm corresponding to a chain with about 10 000 glucopyranose units. Cellulose molecules are linear and are aggregated through van der Waals forces and both intra- and intermolecular hydrogen bonds. In a woody plant cell, the linear cellulose chains referred to as microfibrils are approximately $3.5 \times 10$ nm in cross-sectional dimension and of indeterminate length. The microfibrils have

both crystalline and amorphous regions. Both linear cellulose molecules and the supermolecular microfibrils have a dominant influence on the behavior of wood as a material. A number of structures for the microfibril have been proposed. These models differ primarily in the description of the amorphous or less ordered regions. All the models can be reduced to one of three basic structures [3, 4].

1. "Longitudinally arranged molecules change from one ordered region to the subsequent one, the transition areas being less ordered regions (fringed micelle system)".
2. "The fibrilllar units are individual cords consisting of longitudinally arranged molecules and sequences of ordered and disordered regions".
3. "The ordered regions are packages of chains folded in a longitudinal direction, the areas containing the turns between adjacent chain packages being the less ordered regions".

The molecular aggregations of cellulose in the wood cell wall contribute to its unique polymer properties. For improving the interaction or interfacial adhesion of cellulose with hydrophobic materials (solvents) it is possible to add a surfactant or to chemically modify its surface. The cellulose reactivity or the lack of reactivity depends on its structure. To modify cellulose structure, the highly ordered hydrogen-bonded lattice must be disrupted by swelling or dissolution. The reactive sites on cellulose, which may be derivatized, are the three-hydroxyl groups indicated as C-2, C-3 and C-6 (Fig. 1). C-6 is a primary hydroxyl, which is the most reactive position for esterification reactions while C-2 is the more acidic of the two secondary hydroxyl groups and is the more reactive site for etherification.

Cellulose has a strong affinity to itself and hydroxyl containing materials. Based on the preponderance of hydroxyl functional groups, cellulose is very reactive with water. At common ambient environmental conditions, cellulose will have at least a monomolecular layer and up to several molecular layers of water associated with it [5]. Cellulose is very stable in a variety of solvents and can only be dissolved by the application of strong acids or strong hydrogen bonding solvent systems, usually amine-based. The thermal properties of cellulose are such that the cellulose glass transition temperature is in the range of 200 to 230°C [6], which is close to its thermal decomposition temperature of 260°C.

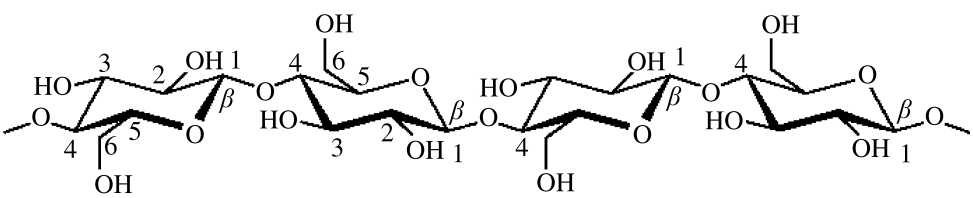


**Figure 1.** Position of hydroxyl groups on cellulose backbone.

Cellulose fibers on the nanoscale are prepared in four different ways: (1) bacterial cellulose nanofibers, (2) cellulose nanofibers by electrospinning, (3) microfibrillated cellulose plant cell fibers and (4) nanorods or cellulose whiskers. Processing techniques have a significant impact on the adhesion properties of the resulting cellulose nanofibers in composite material applications.

## 3. Cellulose Adhesion in Paper

Adhesion in cellulose-based fiber materials, i.e. paper, has long been recognized going back 5000 years when Egyptians invented papyrus parchments [7]. The ease of adhesion that occurs between cellulose fibers has contributed to a globally important industry that is among the largest in the world. Cellulose fiber bonding in paper and related products occurs over a practical length scale ranging from the nanoscale to millimeters, and this topic has received considerable attention over the past 50 years [8]. The adhesion theories that have been examined in the bonding of cellulose fibers in paper include: mechanical interlocking, adsorption or wetting theory, diffusion theory, and the theory of weak boundary layers. Most paper fibers manufactured from wood pulp range in length from 1 to 7 mm depending on the species [7]. The bonding of cellulose fibers in paper relies primarily on hydrogen bonding between the fibers that occurs as the wetted fibers dry in contact with each other, and the bond strength can vary greatly depending on the method(s) used to prepare the fibers including the pulping, bleaching and/or refining process. Hydrogen bonding between fibers requires close proximity between adjacent hydroxyl groups (0.25–0.35 nm). The partial solubility of cellulose in water and the diffusion theory of adhesion have also been reported since refined fibers have a fibrillar structure on the near-molecular-size scale that contributes to adhesion [8]. Mechanical interlocking has not been shown to be important in the bonding of cellulose fibers in paper except for paper in the bone-dry condition [8]. The adsorption of hydrophobic materials on cellulose fibers during papermaking greatly decreases fiber-to-fiber bonding and is related to the weak boundary layer theory of adhesion [9].

## 4. Cellulose Adhesion in Films

The preparation and use of smooth cellulose surfaces has facilitated experimental adhesion studies [10–13] on cellulose. Many researchers have prepared model surfaces of cellulose using spin coating [11, 12, 14], and spin casting [15] processes. Riegler and Sczech [11] prepared molecularly thin, smooth cellulose films on wafer surfaces by spin coating a solution of cellulose dissolved in DMAc/LiCl. The cellulose layers were used to investigate cellulose/cellulose adhesion and their modification by polyelectrolytes. Falt *et al.* [12] prepared films of cellulose II through the dissolution of pulp in *N*-methylmorpholine-*N*-Oxide (NMMO) and diluted it to a specific concentration with dimethylsulfoxide and spin-coated the solution onto an oxidized silicon wafer. They showed that the final thickness of the cellulose

films is dependent on the cellulose concentration of the solution; the temperature of the solution has no effect on the film thickness but affects the surface roughness. Gray and Edgar [13] prepared smooth cellulose I surfaces from suspensions of cellulose nanocrystals obtained from acid hydrolysis of cotton and wood pulp. Eriksson *et al.* [10] prepared three different cellulose surfaces, one crystalline and two surfaces with a lower degree of crystallinity. They studied the adhesion between two cross-linked poly(dimethylsiloxane) (PDMS) surfaces, as well as the adhesion between PDMS and the cellulose surfaces prepared. They determined that the work of adhesion was similar for all three cellulose surfaces, and from contact angle measurements with methylene iodide, it was concluded that dispersion interactions dominated the surface. They also found differences in the adhesion properties between the different degree of crystalline order probably because of the surface groups' ability to orient themselves and participate in specific or nonspecific interactions; a surface with a lower degree of crystalline order has a higher possibility for reorientation of the surface groups.

The different studies performed mainly on cellulose models have been focused on the electrostatic and adsorption or wetting mechanisms of cellulose adhesion.

### *4.1. Electrostatic*

Atomic force microscopy (AFM) has been used to evaluate adhesion properties of cellulose surfaces. Borkovek *et al.* [16] studied the interaction of cellulose layers with negatively charged colloidal silica particles. They found repulsive forces between the silica particles and the cellulose surfaces, which were interpreted quantitatively in terms of electrostatic interactions because of overlap of diffuse layers originating from negatively charged carboxylic groups on the cellulose surface. The authors concluded that nonelectrostatic forces, probably originating from hydrogen bonding, dominate the adsorption of cellulose onto probe surfaces. The electrostatic contribution to desorption forces could be detected only at a high pH, where the silica surface is highly charged. Zhang and Young [17] determined the adhesion properties of acetone extracted cellulose films, which are rich in –OH groups. Both standard silicon nitride tips as well as self-assembled monolayer modified gold-coated tips containing a variety of specific functional groups were used to make the surface analyses. The authors determined that the adhesion force detected with –COOH terminated tips (approx. 34.8 nN) was much larger than that with $–CH_3$ terminated tips (16.7 nN), which was attributed to the hydrogen bonding between –COOH and –OH functional groups. The adhesion force of $–NH_2$ terminated AFM tips on acetone extracted cellulose film was 42.9 nN, the strongest adhesion behavior, because of acid–base interaction was observed after introducing $NH_2$ groups on the surface films (using hydrazine plasma treatment) and using AFM tips terminated with –COOH. Conversely, the adhesion forces were reduced to 17.4 and 19.4 nN after their treatment with argon and oxygen based plasmas, respectively, probably as a result of greatly enhanced surface roughness of the films. Nigmatullin *et al.* [18] determined that the interaction between pure cellulose surfaces in an aqueous

electrolyte solution was dominated by double layer repulsive forces, with the range and magnitude of net force depending on electrolyte concentration. The interaction was attributed to the negative charge of the cellulose surface.

### *4.2. Adsorption or Wettability*

Surface energy or surface wettability as an indication of the adhesion properties of cellulose has been widely studied using techniques that include thin-layer wicking [19], liquid absorption into cellulose pulp sheets [20], powder contact angle analysis [21], contact angle analysis of cellulose films [22, 23], the Whilhelmy technique [24], inverse gas chromatography [25–27] and atomic force microscopy [16, 17, 28]. For surface energy determinations, the results are mainly interpreted in terms of Lifshitz–van der Waals ($\gamma_s^{LW}$) and electron-donor (base, $\gamma_s^-$), and electron-acceptor (acid, $\gamma_s^+$) components of the surface energy. Table 1(a)–(c) show the surface energy components of cellulose presented by different authors. Table 1(a)–(c) indicate that in some cases cellulose surfaces have a lower acid–base component compared to the dispersion component; conversely in other cases cellulose surfaces have a higher acid–base component. The variation in the values obtained could be explained principally because of the specific raw material used (preparation), the surface morphology, the techniques used for the measurements, and in some cases to the relationship of the models used for the calculations of the surface energy. Mota *et al.* [19] determined the surface energy components of three

**Table 1(a).**
Cellulose surface energy components (in mJ/m$^2$)

| Raw material | $\gamma_s^{LW}$ | $\gamma_s^+$ | $\gamma_s^-$ | $\gamma_s^{AB}$ * | $\gamma$ total ($\gamma_s^{LW} + \gamma_s^{AB}$) | Polarity ($\gamma_s^{AB}/\gamma$ total) (%) | Reference |
|---|---|---|---|---|---|---|---|
| Cellulose film | 40 | 2 | 44 | 18.8 | 58.8 | 32 | Forsstrom *et al.* [22] |
| Hydrophobic cellulose | 29 | 0.08 | 4 | 0.57 | 29.6 | 1.9 | Forsstrom *et al.* [22] |
| Cellulose pulps | 35 | 1.2 | 15 | 8.5 | 43.5 | 20 | Pezron *et al.* [20] |
| Cellulose ether films | | | | | | | |
| Hydroxypropyl methylcellulose | 35.8 | 0.15 | 27.2 | 4.0 | 39.9 | 10 | |
| Methylcellulose | 36.3 | 0.04 | 36.7 | 2.4 | 38.7 | 6.3 | Luner and Oh [15] |
| Hydroxypropyl cellulose | 40.2 | 0.11 | 17.2 | 2.8 | 45.0 | 6.4 | |
| Hydroxyethyl cellulose | 44.8 | 0.16 | 40.1 | 5.1 | 49.9 | 10.2 | |

* $\gamma_s^{AB} = 2 \cdot (\gamma_s^+ \gamma_s^-)^{(1/2)}$ (Luner and Toussaint [105]).

**Table 1(b).**
Cellulose surface energy components (in mJ/m$^2$)

| Raw material | $\gamma_s^{LW}$ | $\gamma_s^+$ | $\gamma_s^-$ | $\gamma_s^{AB*}$ | $\gamma$ total ($\gamma_s^{LW} + \gamma_s^{AB}$) | Polarity ($\gamma_s^{AB}/\gamma$ total) (%) | Reference |
|---|---|---|---|---|---|---|---|
| Microcrystalline cellulose at 39°C | 52.3 | – | – | – | – | – | |
| Microgranular cellulose at 39°C | 43.2 | – | – | – | – | – | |
| Microfibrous cellulose at 39°C | 44.3 | – | – | – | – | – | Papirer *et al.* [27] |
| Cotton | 39 | – | – | – | – | – | |

* $\gamma_s^{AB} = 2 \cdot (\gamma_s^+ \gamma_s^-)^{(1/2)}$ (Luner and Toussaint [105]).

**Table 1(c).**
Cellulose surface energy components (in mJ/m$^2$)

| Raw material | $\gamma_s^{LW}$ | $\gamma_s^+$ | $\gamma_s^-$ | $\gamma_s^{AB*}$ | $\gamma$ total ($\gamma_s^{LW} + \gamma_s^{AB}$) | Polarity ($\gamma_s^{AB}/\gamma$ total) (%) | Reference |
|---|---|---|---|---|---|---|---|
| Sigmacell 101, Sigmacell 20 and Avicel 101 | 50–56 | ≈0 | 42–45 | – | – | – | Mota *et al.* [19] |
| Cellulose film | 39.1 | 2 | 39.7 | 17.8 | 56.7 | 31.8 | Luner and Toussaint [105] |
| Cellulose film | 44.6 | 1.2 | 19.4 | 9.6 | 54.2 | 18 | van Oss and Costanzo [106] |
| Viscose, lyocel and modal fibers | 8–8.3 | – | – | 25–25.5 (determined) | 33 | 75 | Persin *et al.* [21] |
| Cellulose from purified cotton | 27.5 | – | – | 41 (determined) | 68.5 | 60 | Berg and Westerlind [24] |
| Highly crystalline cellulose (Avicel) | 29.1 | – | – | 34.8 (determined) | 63.9 | 54.5 | Lee and Luner [107] |

* $\gamma_s^{AB} = 2 \cdot (\gamma_s^+ \gamma_s^-)^{(1/2)}$ (Luner and Toussaint [105]).

celluloses (Sigmacell 101, Sigmacell 20 and Avicel 101) using the thin layer technique and the Washburn equation. Their results indicate that all three celluloses have high apolar ($\gamma_s^{LW}$) and electron donor ($\gamma_s^-$) components, while the electron acceptor component ($\gamma_s^+$) is practically zero. The free energy interactions of cellulose/water/cellulose calculated from the components are positive, regardless of the cellulose crystallinity. This would mean that the cellulose surfaces have a hydrophilic character. However, the work of spreading of water has a small negative

value (3–9 mJ/m$^2$), indicating that the surfaces are slightly hydrophobic. It is believed that the work of spreading better characterizes the hydrophobicity of the surface than the free energy of particle/water/particle interaction, because in the latter case, no electrostatic repulsion is taken into account in the calculations. Pezron *et al.* [20] determined the cellulose pulp surface energy by liquid absorption into cellulose pulp sheets in relation to bacterial adhesion; Berg and Jacob [25] used inverse gas chromatography to determine the surface energy of microcrystalline cellulose and two wood pulp fibers. They determined that all three surfaces exhibited both acidic and basic characteristics, but were predominantly acidic in nature. Papirer *et al.* [27] demonstrated the influence of crystallinity on surface energy values; microcrystalline cellulose showed a significantly higher ($\gamma_s^{LW}$) value (41 mJ/m$^2$) than amorphous cellulose (27.4 mJ/m$^2$). The authors used three different kinds of cellulose (microcrystalline (6.3 m$^2$/g), microgranular (34.5 m$^2$/g) and microfibrous (7 m$^2$/g)). They determined that the dispersion component of surface energy (Table 1(a)–(c)), the acid–base properties, nanomorphology and humidity all influenced these properties. They determined that the flattest surface corresponded to microcrystalline cellulose and therefore the better accessibility of the solid surface to adsorbing molecular probes. Luner and Oh [15] reported surface energy components of cellulose ether films that were lower than cellulose. They determined that the dispersion ($\gamma_s^{LW}$) component of surface energy was almost constant for cellulose ethers as compared with the acid–base component; this was explained based on the theory that the dispersion component of many polymers is independent of their surface chemical composition. That the $\gamma_s^+$ component of cellulose is significantly greater than the cellulose ethers, maybe because of its relatively larger number of free hydroxyl groups.

### *4.3. Hydrophobic* Versus *Hydrophillic*

Yamane *et al.* [23] attempted to clarify the hydrophilic and hydrophobic nature of cellulose based on its structural anisotropy. Regenerated cellulose is known as among the most hydrophilic polymers and the high wettability of cellulose films results from its high density of hydroxyl groups. However, it was also demonstrated that cellulose also interacts with hydrophobic organic solvents (hexane, toluene, dichloromethane). The authors proposed that the hydrophilic behavior of cellulose was due to the location of hydroxyl groups at the equatorial positions of the glucopyranose rings. Conversely, the axial direction of the glucopyranose ring is hydrophobic because atoms of C−H bonds are located on the axial positions of the ring. According to the authors, this suggests that the hydrophobic property of cellulose may be created by structural controls such as reversing the planar orientation.

It is of interest to mention the work performed by Klingenberg and Zauscher [29] who studied the interaction between cellulose surfaces in aqueous solutions using colloidal probe microscopy. They reported that long-range interactions between cellulose surfaces are governed by double-layer forces and, once surfaces are in contact, by osmotic repulsive forces and viscoeleasticity.

## 5. Challenges of Cellulose Adhesion on the Nanoscale

The ease of adhesion between pulp fibers that occurs during papermaking poses challenges to processing cellulose on the nanoscale. The hydrogen bonds present on the surface of nanofibers or nanorods (whiskers) or of cellulose are the key for a better manageability of these new materials to determine future applications. These applications will be strongly dependent on the surface properties of nanocellulosic materials and their capability to be compatible with the matrix in which they are processed.

There are four types of nanocellulose depending on their manner of fabrication. These include: bacterial cellulose, electrospun cellulose, microfibrillated cellulose (MFC) and whiskers of cellulose (nanorods). A review of each of them is presented in the following paragraphs.

### *5.1. Bacterial Cellulose Nanofibers*

Bacterial cellulose is a nanomaterial derived from various strains of *Acetobacter* species [30, 31]; although strains of pseudomonas, *Achrobacter*, *Alcaligene*, *Aerobacter* and *Azotobacter* [32] also can be used to produce cellulose. An in-depth review of cellulose biosynthesis and function in bacteria was presented by Ross *et al.* [33], but a brief description of experimental details is presented here. The *Acetobacter* species is cultivated in a medium containing carbon and nitrogen sources in either a static or shaken environment [31]. However, oxygen is needed for cell division and cellulose synthesis and if oxygen is removed and replaced by pure nitrogen, no cellulose is obtained [34].

The bacterial cellulose is in network form containing pellicles of ribbon shaped cellulose fibrils that are less then 100 nm wide and are made of microfibrils 2–4 nm in diameter [35]. Typical uses for the microbial derived nanocellulose range from medical applications [31], reinforcement in high quality papers [36], diaphragms for electro-acoustic transducers [37], paint additives, coatings, pharmaceuticals and cosmetics [32], and reinforcement for optically transparent films [38].

Wan *et al.* [31] researched the use of bacterial cellulose for reinforcement in medical materials. Poly(vinyl alcohol) (PVA) was mechanically enhanced with the addition of bacterial cellulose. The addition of the bacterial cellulose allowed PVA, which has similar mechanical properties to various biological tissues, to be "tunable" over a broad range allowing the material to closely match various tissues for many medical applications. Nogi *et al.* [38] found that bacterial cellulose nanofibers could be used as reinforcement in optically transparent materials. The ability to reinforce transparent materials is because of its high Young's modulus and tensile strength of 138 and 2 GPa, respectively [39, 40]. Also, bacterial cellulose has a very low thermal expansion of only $0.1 \times 10^{-6}$ $K^{-1}$ [39]. The resin used was acrylic and to maintain transparency, fiber content ranged from 7.4 to 66.1 wt%. The findings indicated that at 7.4 wt% reinforcement the light transmittance was reduced by 2.4% and the thermal expansion coefficient was reduced from $86 \times 10^{-6}$ to $38 \times 10^{-6}$ $K^{-1}$. These findings indicate that bacterial cellulose would make an

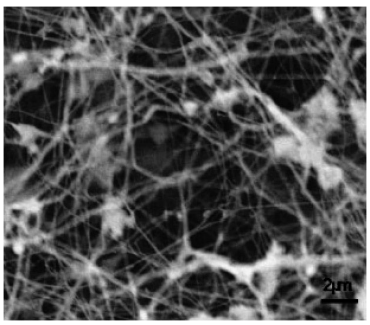


**Figure 2.** Bacterial cellulose nanofibers: SEM image of the outer side (B) of the tubes produced with 100 wt% of oxygen. Magnification 5000× [109]. Reprinted with permission of Wiley-Liss, Inc., a subsidiary of John Wiley & Sons, Inc.

effective nanofiber reinforcement for materials that require a low degree of thermal expansion and are optically transparent.

Bacterial cellulose is also used in hi-fidelity loudspeakers and headphones because of two essential properties: high sonic velocity and low dynamic loss; "it is seen that both frequency response and second harmonic distortion are smoothed and extended to higher frequency regions" [36]. Moreover, bacterial cellulose can be used in acoustic applications because of its high sonic velocity and low dynamic loss properties. "In fact, the sonic velocity of pure film was almost equivalent to those of aluminum and titanium, while the tangent-delta was in a low range, 0.4–0.5" [36].

For all of these applications, the nature of bacterial cellulose provides the special properties that allow the unique materials to be formed. Figure 2 shows how the bacterial cellulose microfibrils look after growth with 100% oxygen.

*5.1.1. Adhesion*

Bacterial cellulose is more ordered than standard cellulose and this order and lack of irregularities leads to both superior reinforcement and thermal expansion properties when used with matrix materials. The inter- and intra-molecular binding and/or adhesion is accomplished through hydrogen bonding. Bacterial cellulose fibers have a degree of polymerization between 2000 and 6000 [36]. This relatively low degree of polymerization may limit the adhesion through interpenetrating networks or mechanical interlocking and, for the most part, the adhesion in composite materials is limited to hydrogen bonding though other mechanisms of adhesion need to be explored.

The elastic modulus of a single bacterial cellulose fiber has been determined by Guhados *et al.* [41]. The researchers worked with an atomic force microscope (AFM) to determine Young's modulus by utilizing a nanoscale 3-point bending apparatus. The nanomechanical testing was done in force-volume mode where the cantilever deflection of the AFM is recorded as a function of vertical sample displacement. Using the 3-point bending method the authors calculated a Young's

modulus of $78 \pm 17$ GPa for bacterial cellulose fibers with diameters ranging from 35 to 90 nm.

### *5.2. Electrospun Cellulose*

Cellulose needs to be in solution form to facilitate electrospinning [42, 43]; some of the solvents used have been *N*-methylmorpholine-*N*-Oxide (NMMO), *N,N*-dimethylacetamide (DMAc) and lithium chloride (LiCl)/*N,N*-dimethyl acetamide (DMAc) [42–46]. In addition to the solvent, other important factors to consider in the intrinsic properties of the solution for the cellulose electrospinning process are the cellulose molecular weight, solution viscosity, net charge density, surface tension of the cellulose solution, and solution conductivity. Some of the operational conditions depend on the applied voltage, spinning temperature, flow rate and distance between the nozzle and collector. The humidity and temperature of the surroundings may also play an important role in determining the morphology and diameter of electrospun nanofibers [47]. The polymer solution must have a concentration high enough to cause polymer entanglements yet not so high that the viscosity prevents polymer motion induced by the electric field. The solution must also have a surface tension low enough, a charge density high enough, and a viscosity high enough to prevent the jet from collapsing into droplets before the solvent has evaporated [48].

Joo *et al.* [44] studied the effect of solvent system, degree of polymerization (DP), processing conditions and post-spinning treatment on the microstruture of sub-micrometer scale, electrospun cellulose fibers. Also, they utilized electrospun cellulose fibers to develop highly oxidized cellulose with $HNO_3/H_3PO_4$ and $NaNO_2$ having a large surface area. The particular interest was to study how the degree of crystallinity of electrospun fibers was influenced by these parameters. Joo *et al.* [44] demonstrated that non-woven mats of submicronized cellulose fibers of 250–750 nm in diameter could be obtained using the electrospinning process. They showed that cellulose fibers obtained from LiCl/DMAc were mostly amorphous, whereas the degree of crystallinity of cellulose fibers from NMMO/water could be controlled by the process conditions. Some pictures of electrospun cellulose are presented in Fig. 3. Liu and Tang [45] used cellulose acetate with the same acetyl concentration (39.8%), but different molecular weights ranging from $3.0 \times 10^4$ to $5.0 \times 10^4$, to prepare cellulose acetate nanofibers and nanofibrous membranes in several conventional solvents such as acetone, acetone/*N,N*-dimethylacetamide (DMAc) and acetone/water. They produced nanofibers with mean diameters less than 265 nm, but nanofibers from low molecular weight cellulose acetate had a larger amount of spindle-like beads on fibers and a broader fiber size distribution compared to those produced from high molecular weight which showed uniform and smooth fiber structure without defects. Joo and co-workers [42] obtained cellulose nonwoven mats of submicrometer-sized fibers (150–500 nm in diameter) by electrospinning cellulose solutions. The solvent system used was based on lithium chloride (LiCl) and *N,N*-dimethylacetamide (DMAc). They evaluated the effect of

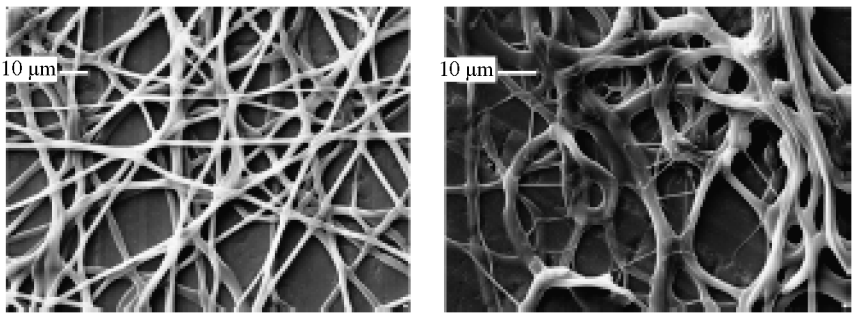


**Figure 3.** SEM images of electrospun fibers from 9 wt% DP210 cellulose/NMMO/water solution with a rotating collector at: (a) 1.2 rpm and (b) 6 rpm. Flow rate was kept at 0.03 ml/min [44]. Reprinted with permission from Elsevier.

temperature of the collector, type of collector (aluminum mesh and cellulose filter media), and post-spinning treatment, such as coagulation with water, on the morphology of electrospun fibers. Ethyl cellulose has also been used to study the diameter distribution and surface morphology of electrospun nanofibers previously dissolved in a multicomponent solvent system (tetrahydrofuran, THF, and *N,N*-dimethylacetamide, DMAc) [49].

Walkenstrom *et al.* [43] used electrospinning to process mixtures of poly (ethylene oxide) (PEO) and cellulose derivatives of carboxymethylcellulose (CMC) sodium salt, hyroxypropylmethylcellulose (HPMC), methylcellulose (MC), and enzymatically treated cellulose. They found that the substitution pattern of carboxymethyl groups on the CMC derivatives proved to be crucial for the appearance of the nanoweb as well as for the morphology of individual nanofibers.

Electrospun fibers have been successfully used for reinforced thermoplastic polymers [50]. Fink and Ganster [50] developed a double pultrusion technique for compounding thermoplastic polymers and electrospun fibers (from viscose and lyocell) for injection moulding applications. They increased the final mechanical properties of the composites up to three times compared to the initial matrix.

### *5.2.1. Adhesion*

The surface characteristics of the electrospun cellulose fibers are strongly dependent on the solvent used to dissolve the cellulose. It is known that to dissolve cellulose without chemical modification or derivatization is difficult because of the molecule stiffness and close chain packing *via* numerous intermolecular and intramolecular hydrogen bonds in the cellulose [51]. As the process of cellulose dissolution is usually connected with H-bond formation between the cellulose hydroxyl groups and solvent molecules, one of the most important criteria of dissolving ability of any solvent is the value of interaction energy of this solvent with cellulose which should be higher than the energy of intermolecular H-bonds in cellulose itself [52]. An analysis of cellulose surface characteristics after the electrospinning process was performed by Liu and Tang [45]. They made water contact angle measurements on

cellulose acetate electrospun fibers and suggested that the orientation of hydrophobic and hydrophilic groups on the outermost fiber surface changed when the fiber size was reduced to the nanometer range.

### *5.3. Microfibrillated Cellulose*

Microfibrillated cellulose (MFC) is a material derived by disintegrating digested cellulose through a homogenizing process, exposing the underlying microfibrils. This new morphology was developed by Turbak *et al.* [53] in the early 1980s. This process usually starts with wood pulp; however, Dufresne *et al.* [54], describe how microfibrillated cellulose can be extracted from sugar beets. Regardless of the starting material, the process always involves a homogenization process. Nakagaito and Yano [55] describe the homogenizing process as subjecting the cellulose to a reciprocating motion producing a high pressure drop resulting in shearing and impact forces. The shearing and impact forces are responsible for exposing the substructural cellulose microfibrils.

Through the homogenization process, the cellulose bundles are split and degraded leaving microfibrillated cellulose strands with dimensions of 10–100 nm [30]. Elementary kraft fibers are on the order of 10's of μm's wide and are rod like [55]; whereas MFC is a network of interconnected microfibrils with little order on the nanometer scale, Fig. 4. Through the homogenization process the ratio of surface area to volume for the fibers is increased dramatically.

Nakagaito and Yano [56] researched phenolic resin reinforced composites where the composite mats had varying resin content. The MFC was passed through a high

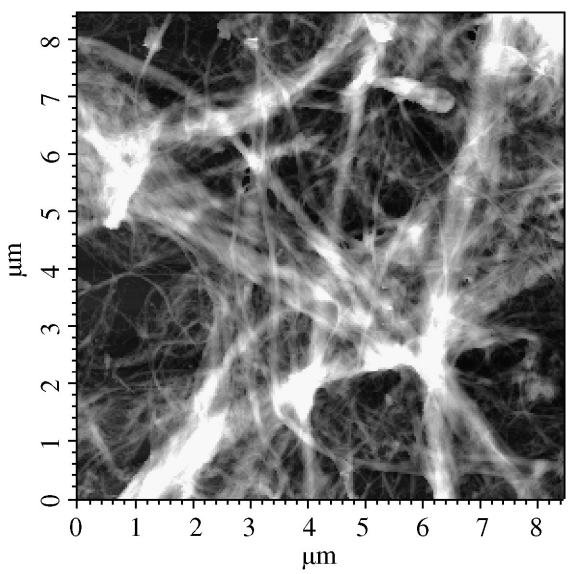


**Figure 4.** AFM image of MFC (homogenized 1 time) (Ryan Lena, Research Experience for Undergraduates, Forest Bioproducts Research Initiative, University of Maine, unpublished).

pressure homogenizer 2, 6, 14, 22 and 30 times creating MFC of varying degree of fibrillation. Their findings indicated that no strength improvements were developed until at least 16 passes through the homogenizer. Their hypothesis for the strength increase due to increased homogenization was that increased homogenization minimized the number of weaker spots that would act as crack initiators. Another hypothesis presented is that bond density is increased and the increase in bond density inhibits crack formation.

Nakagaito and Yano [55] did more work with the MFC composites this time working with phenol-formaldehyde (PF) resins. In both studies, kraft pulp was used to make the MFC. In this study all the pulp was homogenized 15 times, the minimum found previously to improve reinforcement properties. The PF resins were reinforced with both pulp and MFC. The findings from this study showed that the Young's modulus of both the pulp based and MFC-based composites were similar in the range of 18–19 GPa; however, the bending strength peaked at 370 and 260 MPa for the MFC and pulp reinforced composites, respectively.

Microfibrillated cellulose, and cellulose in general, has a very low thermal expansion coefficient. Nishino *et al.* [39] worked with all cellulose composites. The all cellulose composites they made had an extremely low thermal expansion coefficient, "apparently almost no thermal expansion or contraction; the $\alpha$ value of the composite was about $10^{-7}$ $K^{-1}$, which is much lower than those of metals (for example, Fe: $11.8 \times 10^{-6}$ $K^{-1}$, Si: $2.49 \times 10^{-6}$ $K^{-1}$)".

Microfibrillated cellulose has been shown to be a performance enhancer when added to composite materials. Okubo *et al.* [57] fabricated a poly(lactic acid) (PLA), bamboo reinforced, composite material. Three-point bending tests, microdrop tests, fracture toughness tests, and bamboo fiber embedded tests were conducted to evaluate mechanical properties. The findings indicated that three-point bending strength and fracture toughness were improved by adding MFC and that MFC fibers entangled onto the bamboo reinforcement preventing crack formation and/or propagation.

MFC has been converted in an attempt to improve composite performance by reducing its hydrophilicity. Andresen *et al.* [65] describe some of the methods used in the literature [58–64] and then present their findings. They surface sized MFC with chlorodimethylisopropylsilane. The sizing was accomplished by grafting and then the resulting modified MFC was analyzed by FT-IR, contact angle analysis, X-ray photoelectron spectroscopy, atomic force microscopy, transmission electron microscopy, and white light interferometry. Their results indicated that too little sizing had only a negligible effect on the hydrophobicity and too much caused solubilization of the MFC. They found that a degree of surface substitution between 0.6 and 1 resulted in a hydrophobic MFC that could be dispersed without agglomeration in organic solvents.

*5.3.1. Adhesion*

The interactions that take place in a composite between the reinforcement and the matrix determine how strong the reinforced material will be Azizi Samir *et al.* [66]

worked with both microfibrils of cellulose and cellulose whiskers to compare the reinforcement properties for these two types of cellulose. Cellulose was exposed to sulfuric acid baths at 40°C for 35 minutes. Two sulfuric acid baths were used: one at 20 wt% and one at 60 wt%. The polymer used was latex reinforced with 6 wt% fiber either untreated or treated in one of the sulfuric acid baths. Results from the study showed that the tensile strength and tensile modulus increased when the cellulosic fibers were added; however, the highest values were found for the microfibril cellulose with no acid treatments. The elongation at break decreased for the material when the cellulosic fibers were added and this is hypothesized to be due to the entanglement of the cellulosic fibers. For the reinforced material, the elongation at break increased as a function of acid hydrolysis strength. All of this is an indication of the significance of entanglement in the overall macroscopic physical properties of the cellulosic reinforced composites.

The hydrogen bonding that takes place between the nanocellulosic materials is well known but the study mentioned above demonstrates how important entanglements are for the microfibrillated cellulosic materials.

### *5.4. Cellulose Nanorods or Whiskers of Cellulose*

Whiskers of cellulose, the needle-like structure of the cellulose crystallite, have been mainly studied for their liquid crystalline behavior in concentrated aqueous suspensions [65, 67–69] and for their reinforcing effect when added to a polymeric matrix giving rise to very strong and tough percolating networks of hydrogen bonded whiskers [70–76]. Whiskers of cellulose are renewable materials which possess high availability, light weight and high mechanical properties. They consist of slender parallelepiped rods and, depending on their origin, the lateral dimensions range from about 2–50 nm in diameter for length than can reach several tens of micrometers [77]. According to these dimensions, they possess high aspect ratios and high specific surface area of about 150 $m^2/g$ [78]. See an example of whiskers of cellulose in Fig. 5 [104].

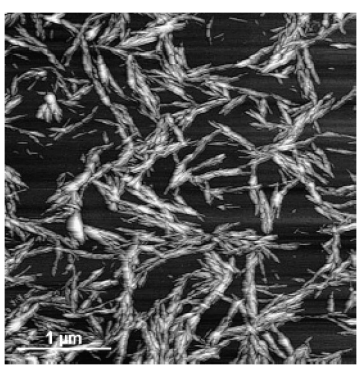


**Figure 5.** AFM topography image of cellulose nanowhiskers from a dried water suspension [104].

**Table 2.**
Characteristics of whiskers of cellulose from different sources [77, 78, 82]

| Cellulose source | Length (nm) | Cross section (nm) |
|---|---|---|
| Tunicate* | 100–several microns | 15 |
| Algal (Valonia) | >1000 | 10–20 |
| Bacterial | 100–several microns | 5–10 by 30–50 |
| Wheat straw | 220 | 5 |
| Cotton | 200–350 | 5–15 |
| Wood | 100–300 | 3–5 |
| Sugar beet pulp | 210 | 15 |

* Marine animal from the Mediterranean Sea.

Several raw materials have been used for producing whiskers of cellulose. These include sugar beet pulp, tunicin from tunicates (a sea animal) [71, 79, 80], mantle of the tunicates [81], valonia, sulphite wood pulp [82, 83], microfibrilated cellulose from kraft pulp [55], wheat straw [84], cotton filter paper [85, 86], bacterial cellulose [62], sisal [87], kraft pulp, hemp, flax [88] and microcrystalline cellulose (MCC) [89]. Some sources for obtaining cellulose nanocrystals and their characteristics are listed in Table 2. The method primarily utilized for obtaining the whiskers has been acid hydrolysis, which consists basically in removing the amorphous regions present in the cellulose fibrils leaving the crystalline regions intact; therefore, the dimensions of the cellulose whiskers obtained after hydrolysis are mainly dependent on the percentage of amorphous regions that varies for each organism. Traditionally the yields of cellulose whiskers by acid hydrolysis have been quite low (2–3%) [90]; however, in a recent study the process was optimized to reach yields up 30% and suspensions of nanocrystals with a length between 200 and 400 nm and a width less than 10 nm [89].

Hydrochloric acid also has been used for obtaining cellulose whiskers; however, the use of sulfuric acid leads to more stable whiskers aqueous suspensions [74, 78, 91, 92] because the whiskers present a higher negative charge on their surface compared with those prepared with HCl [93]; the repulsion forces are then also higher and the flocculation between the nanoparticles is reduced. Another way to achieve charged whiskers consists of the oxidation of the whiskers surface [94, 95] or through an acylation process [96].

Nanocomposite films either by film casting (water evaporation) or by freeze drying, followed by classical compression or extrusion, have been prepared to study cellulose whiskers reinforcing properties in thermoplastics [97–100] or thermoset matrices [72]. Water suspensions of whiskers have been preferred in nanocomposite films because of their high stability and the expected high level of dispersion of the whiskers within the host matrix in the resulting films. This behavior, however, restricts the choice of the matrix to hydrosoluble polymers. The utilization of latexes, which allows the use of hydrophobic polymers as matrix, is a practical

alternative and ensures a good dispersion level of the filler required for homogeneous composite processing [79, 98]. The simplest technique to process a composite material from latex and aqueous suspension of whiskers consists in mixing and casting the two aqueous suspensions. A solid nanocomposite film can be then obtained by water evaporation and particle coalescence at a temperature higher than the glass transition temperature of the matrix [77]. Some polymer latexes used for film nanocomposites include those obtained by copolymerization of styrene and butyl acrylate [77, 79, 101] and poly(hydroxyoctanoate). Another alternative to processing nanocomposites using whiskers consists in dispersing them in an organic medium. In this case, for improving compatibility between the polar whiskers and apolar matrices, the addition of surfactants and chemical modification of the whiskers have been proposed [80, 81, 86]. Surface modification involves reacting the hydroxyl groups on the surface of whiskers and in this way Grunert and Winter [62], for instance, used trimethylsilylation for reducing the hydrophilicity of the whisker surfaces. The use of surfactants improves compatibility, but large amounts of them are required because of the high specific area of the whiskers [76]. Dispersion of cellulose whiskers has also been studied using polar organic solvents [79, 102]. Dufresne *et al.* [79] dispersed cellulose whiskers from tunicin in an organic solvent (*N,N*-dimethylformamide, DMF) without addition of a surfactant or any chemical modification. Gray *et al.* [102] dispersed whiskers of cellulose in DMF and in dimethylsulfoxide (DMSO) and prepared nanocomposite films. Cavaillé *et al.* [72] processed and characterized thermosetting nanocomposites using aqueous suspensions of microcrystalline cellulose and an epoxy matrix. They concluded that the reinforcing effect was due to the strong interactions existing between the cellulose whiskers and the epoxy network and the creation of a percolating network linked by H-bonds between cellulose fibers.

*5.4.1. Adhesion*

Whiskers of cellulose have a hydroxyl-rich surface and in contact with relatively polar surfaces (like ester functional groups present in PVAc) will form hydrogen bonds that are expected to strengthen the interface significantly with a positive impact on the mechanical properties of the material. It has been previously shown that the cellulose whiskers form a rigid three-dimensional network above whisker percolation because of hydrogen bond formation between the individual whiskers [93]. Some chemical modifications of the surface of cellulose whiskers that increase its hydrophobicity include surface acylation [96] and silylation [61, 65]. Such modification allows the whiskers to disperse in solvents of low polarity.

A summary with the main properties of nanocellulose prepared by different processes is presented in Table 3.

## 6. Summary and Discussion

A short summary and discussion of the four types of nanocellulose reviewed is presented as follows: (1) Bacterial cellulose forms a perfectly ordered fibril structure.

**Table 3.**
Properties of nanocellulose obtained using different processing methods

| | Raw material | Processing method | Main properties | | | |
|---|---|---|---|---|---|---|
| | | | Young's modulus (GPa) | Elasticity modulus (GPa) | Tensile strength (GPa) | Thermal properties |
| Bacterial cellulose nanofibers | Bacteria, nutrients | Bacterial cultivation | 138 (Nishino *et al.* [39]) | $78 \pm 17$ (Guhados *et al.* [41]) | 2 (Page and El-Hosseiny [40]) | $0.1 \times 10^{-6}$ $K^{-1}$ (Nishino *et al.* [39]) |
| Electrospun cellulose fibers* | Dissolved cellulose | Electrospinning process | n.a. | 11 (Fink and Ganster [50]) | 0.33 (Fink and Ganster [50]) | n.a. |
| Cellulose microfibrillated (MFC) | Digested cellulose | Homogenizing | n.a. | n.a. | n.a. | n.a. |
| Whiskers of cellulose | Various cellulose sources [55, 62, 71, 79–88] | Acid hydrolysis | 130–250 (Nishino *et al.* [108]) | n.a. | 0.8–10 (Nishino *et al.* [108]) | n.a. |

n.a.: not available.
* For Viscose sliver [50].

Expectations would be that this structure would outperform other less ordered fibril types. The findings of Nakagaito *et al.* [30] indicate that microbial cellulose has an advantage over other nanoscale celluloses because of its regularity and continuous alignment. (2) The interest in electrospinning as a novel cellulose fiber production technology has increased over the past 5 years. Through the electrospinning process it is possible to produce fibers from 50 to 500 nm in diameter, with high specific surface area and small pore size. In this way, several solvents for dissolving cellulose have been studied; however, there is still no consensus about the most appropriate cellulose solvent considering economics, safety and operational issues. Also, although efforts have been made to characterize the surface chemistry of films or membranes prepared with electrospun fibers, the surface chemistry of the individual electrospun fibers has not been clearly determined. (3) Microfibrillated cellulose is fabricated by mechanical action called homogenization and results in different properties based on the number of homogenization passes. These homogenization passes make strands of nanocellulose fibrils that are used for reinforcement in matrix materials. The cellulose microfibrils form an entangled network of fibers which is shown to be an adhesion mechanism in MFC reinforced composites. (4) Finally, whiskers of cellulose have been extensively studied for more than 10 years.

Most of the research has been focused on the preparation of cellulose whiskers (using different sources), characterization and their incorporation in thermoplastic, thermosetting and/or biodegradable matrices (PLA) for nanocomposite production. However, applications of cellulose whisker nanocomposites have not achieved commercial viability. The traditional way to obtain cellulose whiskers is through a hydrolysis process which has been optimized from 2–3% yield to 30% yield (of initial weight). The interface between the polymer matrix and whiskers of cellulose and the dispersion quality of the nanocellulose in polymer matrices still need to be optimized for better interactions and improvement of the mechanical properties of the final nanocomposites.

## 7. Conclusions–Future Directions

As a generalized conclusion, cellulose adhesion appears to be dominated by hydrogen bonding across the length scales from macroscopic to nanoscopic. Future work should utilize analytical techniques such as inverse gas chromatography and atomic force microscopy to determine surface energy and adhesion characteristics of nanocellulose fibers. From such studies, surface sizing needs can be determined for nanocellulose to aid in dispersion and improve interfacial compatibility in nanocomposites to maximize material properties. Although some research has been performed to characterize cellulose at a nanolevel, through the preparation of molecularly smooth cellulose films, it is necessary to continue research in this area to obtain a better understanding of the adhesion interactions beyond hydrogen bonding including mechanical interlocking, interpenetrating networks, and covalent linkages on a fundamental level to improve interfacial properties with thermoplastics, thermosets and biopolymers. A number of studies have promoted the properties of nanocomposites such as lightweight, strength, biodegradability (depending on the matrix used), etc., however, only a few specific applications have been presented. Therefore, future work should focus on real world applications where the properties and/or economic justifications are better than existing materials.

According to a Vision and Technology Roadmap developed by Agenda 2020 (103) some future directions in the area of nanocomposites using cellulose and lignocellulose are:

- Modification of the side chains of inorganics, such as siloxanes, silanes, or sodium silicates, to link the cellulose fibers through Si−OH bonds forming an organic/inorganic matrix.
- Development of systems that simulate the growth of cellulose in trees or plants that can be accomplished on an industrial scale.
- Use of cellulose nanocrystals for reinforcement of other matrix materials.
- Modification of the side chains of cellulose to further enhance self-assembly.

The research needs for nanocellulose adhesion ensure a bright future for this important, renewable polymer resource.

*Acknowledgements*

Funding for this work was provided by the Maine Agricultural and Forestry Experiment Station McIntire-Stennis project ME09615-08, "Micro- and nanocellulose fiber filled engineering thermoplastic composites"; Federal Highway Administration (FHWA), Contract #DTFH61-06-C-0064, "The Structural Use of WPCs in Transportation Applications", and the National Science Foundation (NSF) under Grant No. EPS-05-54545. The AFM picture in Fig. 3 came from an NSF-Research Experience for Undergraduate project by Ryan Lena, Grant No. EEC-0648793, "Explore It! Building the Next Generation of Sustainable Energy Researchers".

## References

1. T. H. Wegner and P. E. Jones, *Cellulose* **13**, 115–118 (2006).
2. E. Sjöström, *Wood Chemistry: Fundamentals and Applications*. Academic Press, San Diego, California (1981).
3. A. Chakraborty, M. Sain and M. Kortschot, in: *Cellulose Nanocomposites: Processing, Characterization and Properties*, K. Oksman and M. Sain (Eds), pp. 169–186. American Chemical Society, Washington, DC (2005).
4. D. Fengel and G. Wegener, *Wood: Chemistry, Ultrastructure, Reactions*. De Gruyter, Berlin (1998).
5. Ch. Skaar, *Wood–Water Relations* (Springer Series in Wood Science). Springer Verlag, New York, NY (1988).
6. D. A. I. Goring, *Pulp Paper Mag. Can.* **64**, T517–T527 (Dec. 1963).
7. C. J. Biermann, *Essentials of Pulping and Papermaking*. Academic Press, New York, NY (1993).
8. J. P. Casey (Ed.), *Pulp and Paper Chemistry and Technology*, Vol. 2, 3rd edn. Wiley-Interscience, New York, NY (1980).
9. J. J. Bikerman, *Ind. Eng. Chem.* **59**, 40–44 (1967).
10. L. Wågberg, M. Eriksson and S. Notley, *Biomacromolecules* **8**, 912–919 (2007).
11. H. Riegler and R. J. Sczech, *J. Colloid Interface Sci.* **301**, 376–385 (2006).
12. S. Fält, E. L. Wågberg, E. L. Vesterlind and P. T. Larsson, *Cellulose* **11**, 151–162 (2004).
13. D. G. Gray and C. D. Edgar, *Cellulose* **10**, 299–306 (2003).
14. E. Kontturi, P. C. Thune and J. W. Niemantsverdriet, *Polymer* **44**, 3621–3625 (2003).
15. P. E. Luner and E. Oh, *Colloids Surfaces A* **181**, 31–48 (2001).
16. M. Borkovek, I. Radtchenko and G. Papastavrou, *Biomacromolecules* **6**, 3057–3066 (2005).
17. X. Zhang and R. Young, *Mater. Res. Soc. Symp. Proc.* **586**, 157–162 (2000).
18. R. Nigmatullin, R. Lovitt, C. Wright, M. Linder, T. Nakari-Setala and M. Gama, *Colloids Surfaces B* **35**, 125–135 (2004).
19. M. Mota, F. Dourado, F. M. Gama and E. Chibowski, *J. Adhesion Sci. Technol.* **12**, 1081–1090 (1998).
20. I. Pezron, A. Rochex, J. M. Lebeault and D. Clausse, *J. Dispersion Sci. Technol.* **25**, 781–787 (2004).

21. Z. Persin, K. Stana-Kleinschek, M. Sfiligoj-Smole, T. Kreze and V. Ribitsch, *Textile Res. J.* **74**, 55–62 (2004).
22. J. Forsstrom, M. Eriksson and L. Wagberg, *J. Adhesion Sci. Technol.* **19**, 783–798 (2005).
23. C. Yamane, T. Aoyagi, M. Ago, K. Sato, K. Okajima and T. Takahashi, *Polym. J.* **38**, 819–826 (2006).
24. J. C. Berg and B. S. Westerlind, *J. Appl. Polym. Sci.* **36**, 523–534 (1988).
25. J. C. Berg and P. N. Jacob, *Langmuir* **10**, 3086–3093 (1994).
26. A. Lundqvist and L. Odberg, in: *Fundamentals of Papermaking Materials* **2**, 751–769. Pira International Ltd. (1997).
27. E. Papirer, E. Brendle, H. Balard and C. Vergelati, *J. Adhesion Sci. Technol.* **14**, 321–337 (2000).
28. A. Pietak, S. Korte, E. Tan, A. Downard and M. P. Staiger, *Appl. Surf. Sci.* **253**, 3627–3635 (2007).
29. D. J. Klingenberg and S. Zauscher, *J. Colloid Interface Sci.* **229**, 497–510 (2000).
30. A. N. Nakagaito, S. Iwamoto and H. Yano, *Appl. Phys. A* **80**, 93–97 (2005).
31. W. K. Wan, J. L. Hutter, L. Millon and G. Guhados, *ACS Symposium Series N°*938, 221–241 (2005).
32. D. Byrom, in: *Biomaterials: Novel Materials from Biological Sources*, D. Byrom (Ed.), p. 265–266. Macmillian Publishers Ltd., UK (1991).
33. P. Ross, R. Mayer and M. Benziman, *Microbiological Reviews* **55**, 35–58 (March, 1991).
34. M. Schramm, Z. Gromet and S. Hestrin, *Biochemical J.* **67**, 669–679 (1957).
35. S. Yamanaka, K. Watanabe, N. Kitamura, M. Iguchi, S. Mitsuhasi, Y. Nishi and M. Uryu, *J. Mater. Sci.* **24**, 3141 (1989).
36. M. Iguchi, S. Yamanaka and A. Budhiono, *J. Mater. Sci.* **35**, 261–270 (2000).
37. Y. Nishi, M. Uryu, S. Yamanaka, K. Watanabe, N. Kitamura, M. Iguchi and S. Mitsuhasi, *J. Mater. Sci.* **25**, 2997 (1990).
38. M. Nogi, S. Ifuku, K. Abe, K. Handa, A. N. Nakagaito and H. Yano, *Appl. Phys. Lett.* **88**, 133124 (2006).
39. T. Nishino, I. Matsuda and K. Hirao, *Macromolecules* **37**, 7683 (2004).
40. D. H. Page and F. El-Hosseiny, *Pulp Pap Canada* **9**, TR99–T100 (1983).
41. G. Guhados, W. Wan and J. L. Hutter, *Langmuir* **21**, 6642–6646 (2005).
42. Y. L. Joo, C.-W. Kim, M. Frey and M. Marquez, *J. Polym. Sci. Part B: Polym. Phys.* **43**, 1673–1683 (2005).
43. P. Walkenstrom, A. Frenot and M. W. Henriksson, *J. Appl. Polym. Sci.* **103**, 1473–1482 (2007).
44. Y. L. Joo, C.-W. Kim, D.-S. Kim, S.-Y. Kang and M. Marquez, *Polymer* **47**, 5097–5107 (2006).
45. H. Liu and C. Tang, *Polym. J.* **39**, 65–72 (2007).
46. P. Kulpinski, *J. Appl. Polym. Sci.* **98**, 1855–1859 (2005).
47. Y. Xia and D. Li, *Adv. Mater.* **16**, 1151–1170 (2004).
48. I. S. Chronakis and A. Frenot, *Curr. Opin. Colloid Interface Sci.* **8**, 64–75 (2003).
49. Y. Huang, X. Wu, L. Wang and H. Yu, *J. Appl. Polym. Sci.* **97**, 1292–1297 (2005).
50. H.-P. Fink and J. Ganster, *Cellulose* **13**, 271–280 (2006).
51. J. Hong and Y. Kuo, *Polym. Adv. Technol.* **16**, 425–428 (2005).
52. A. M. Bochek and L. M. Kalyuzhnaya, *Russ. J. Appl. Chem.* **75**, 989–993 (2002).
53. A. F. Turbak, F. W. Snyder and K. R. Sandberg, *J. Appl. Polym. Sci.: Appl. Polym. Symp.* **37**, 815 (1983).
54. M. A. S. Azizi Samir, A. Dufresne, F. Alloin and M. Paillet, *Macromolecules* **37**, 4313–4316 (2004).
55. A. N. Nakagaito and H. Yano, *Appl. Phys. A* **80**, 155–159 (2005).

56. A. N. Nakagaito and H. Yano, *Appl. Phys. A* **78**, 547–552 (2004).
57. K. Okubo, T. Fujii and N. Yamashita, *JSME Series A* **48**, 199–204 (2005).
58. J. F. Sassi and H. Chanzy, *Cellulose* **2**, 111–127 (1995).
59. J.-Y. Cavaille, H. Chanzy, E. Fleury and J.-F. Sassi, US Patent 6 117 54 (1997).
60. M. J. Cash, A. N. Chan, H. T. Conner, P. J. Cowan, R. A. Gelman, K. M. Lusvardi, S. A. Thompson and F. P. Tise, US Patent 6 602 994 (1999).
61. C. Gousse, H. Chanzy, G. Excoffier, L. Soubeyrand and E. Fleury, *Polymer* **43**, 2645–2651 (2002).
62. M. Grunert and W. T. Winter, *J. Polym. Environ.* **10**, 27–30 (2002).
63. D. Y. Kim, Y. Nishiyama and K. Shigenori, *Cellulose* **9**, 361–367 (2002).
64. C. Gousse, H. Chanzy, M. L. Cerrada and E. Fleury, *Polymer* **45**, 1569–1575 (2004).
65. M. Andresen, L. Johansson, B. Tanem and P. Stenius, *Cellulose* **13**, 665–667 (2006).
66. M. A. S. Azizi Samir, F. Alloin, J. Y. Sanchez and A. Dufresne, *Polymer* **45**, 4033 (2004).
67. S. Matthews, K. Fleming, D. Gray and S. Prasannan, *J. Am. Chem. Soc.* **122**, 5224–5225 (2000).
68. D. G. Gray and W. Chen, *Langmuir* **18**, 633–637 (2002).
69. D. G. Gray and E. D. Cranston, *Sci. Technol. Adv. Mater.* **7**, 319–321 (2006).
70. J. Y. Cavaillé, V. Favier and H. Chanzy, *Macromolecules* **28**, 6365–6367 (1995).
71. V. Favier, J. Y. Cavaillé, G. R. Canova, H. Chanzy, A. Dufresne and C. Gauthier, *Polym. Adv. Technol.* **6**, 351–355 (1995).
72. J. Y. Cavaillé, M. M. Ruiz, A. Dufresne, J. F. Gerard and C. Graillat, *Composite Interfaces* **7**, 117–131 (2000).
73. W. Gindl and J. Keckes, *Polymer* **46**, 10221–10225 (2005).
74. N. A. Kotov, P. Podsiadlo, S. Y. Choi, B. Shim, J. Lee and M. Cuddihy, *Biomacromolecules* **6**, 2914–2918 (2005).
75. K. Oksman and L. Petersson, *Composites Sci. Technol.* **66**, 2187–2196 (2006).
76. L. Heux, G. Chauve and C. Bonini, *Langmuir* **16**, 8210–8212 (2000).
77. A. Dufresne, *J. Nanosci. Nanotechnol.* **6**, 322–330 (2006).
78. L. Chazeau, P. Terech and J. Y. Cavaillé, *Macromolecules* **32**, 1872–1875 (1999).
79. A. Dufresne, M. A. S. Azizi Samir, F. Alloin, J. Y. Sanchez and N. El Kissi, *Macromolecules* **37**, 1386–1393 (2004).
80. L. Heux, N. Ljungberg and J. Y. Cavaillé, *Polymer* **47**, 6285–6292 (2006).
81. L. Heux, C. Bonini, J. Y. Cavaille, P. Linder, C. Dewhurst and P. Terech, *Langmuir* **18**, 3311–3314 (2002).
82. D. G. Gray, S. Beck-Candanedo and M. Roman, *Biomacromolecules* **6**, 1048–1054 (2005).
83. T. Zimmermann, E. Pohler and T. Geiger, *Adv. Eng. Mater.* **6**, 754–761 (2004).
84. A. Dufresne, W. Helbert and J. Y. Cavaillé, *Polym. Composites* **17**, 604–611 (1996).
85. R. Borsali, T. Ebeling, M. Paillet, O. Diat, A. Dufresne, J. Y. Cavaille and H. Chanzy, *Langmuir* **15**, 6123–6126 (1999).
86. M. M. De Souza Lima, J. T. Wong, M. Paillet, R. Borsali and R. Pecora, *Langmuir* **19**, 24–29 (2003).
87. A. Dufresne, N. Garcia de Rodriguez and W. Thielemans, *Cellulose* **13**, 261–270 (2006).
88. A. Bhatnagar and M. Sain, *J. Reinf. Plast. Composites* **24**, 1259–1268 (2005).
89. C. Oksman, D. Bondeson and A. Mathew, *Cellulose* **13**, 171–180 (2006).
90. B. Dawson-Andoh, Enhancement of commercial competitiveness of appalachian hardwoods through advanced technologies (2005). http://www.forestry.caf.wvu.edu/WVU_Final.pdf
91. J. Araki, M. Wada, S. Kuga and T. Okano, *Colloids Surfaces A* **142**, 75–82 (1998).
92. R. Borsali and M. M. De Souza Lima, *Macromol. Rapid Commun.* **25**, 771–787 (2004).

93. M. A. S. Azizi Samir, A. Dufresne and F. Alloin, *Biomacromolecules* **6**, 612–626 (2005).
94. J. Araki, M. Wada and S. Kuga, *Langmuir* **17**, 21–27 (2001).
95. M. R. Vignon, Y. Habibi and H. Chanzy, *Cellulose* **13**, 679–687 (2006).
96. S. Kuga, H. Yuan, Y. Nishiyama and M. Wada, *Biomacromolecules* **7**, 696–700 (2006).
97. P. Hajji, V. Favier, C. Gauthier and G. Vigier, *Polym. Composites* **17**, 612–619 (1996).
98. J. Y. Cavaillé, L. Chazeau, G. Canova, R. Dendievel and B. Boutherin, *J. Appl. Polym. Sci.* **71**, 1797–1808 (1999).
99. J. Y. Cavaillé, L. Chazeau and M. Paillet, *J. Polym. Sci. Part B Polym. Phys.* **37**, 2151–2164 (1999).
100. J. Y. Cavaillé, L. Chazeau and J. Perez, *J. Polym. Sci. Part B Polym. Phys.* **38**, 383–392 (2000).
101. V. Favier, G. R. Canova, J. Y. Cavaille, H. Chanza, A. Dufresne and C. Gauthier, *Polym. Advan. Technol.* **6**, 351–355 (2003).
102. D. Gray, D. Viet and S. Beck-Candanedo, *Cellulose* **14**, 109–113 (2007).
103. Nanotechnology for the Forest Product Industry, Vision and Technology Roadmap. www.nanotechforest.org
104. K. Oskman and I. Kvien, *Appl. Phys. A* **87**, 641–643 (2007).
105. P. Luner and A. F. Toussaint, *J. Adhesion Sci. Technol.* **7**, 635–648 (1993).
106. C. J. van Oss and P. M. Costanzo, *J. Adhesion Sci. Technol.* **6**, 477–487 (1992).
107. S. B. Lee and P. Luner, *Tappi* **55**, 116–121 (1972).
108. T. Nishino, K. Takano and K. Nakamae, *J. Polym. Sci. Part B Polym. Phys.* **33**, 1647 (1995).
109. A. Bodin, H. Backdahl, H. Fink, L. Gustafsson, B. Risberg and P. Gatenholm, *Biotechnol. Bioeng.* **97**, 425–434 (2007).